



## Dendrite-Free Electrochemical Deposition of Li–Na Alloys from an Ionic Liquid Electrolyte

Kevin P. Doyle, Christopher M. Lang,\* Ketack Kim,\* and Paul A. Kohl\*\*z

Chemical and Biomolecular Engineering, Georgia Institute of Technology, Atlanta, Georgia 30332-0100, USA

The deposition of Li–Na alloys from an ionic liquid medium has been demonstrated and evaluated with respect to dendrite growth, oxidation potential, and stability. The maximum coulombic efficiency for the reoxidation of the Li–Na alloy was found to be 91%. The conductivity of the ionic liquid medium containing the alloy salts was 364–466  $\mu\text{S}/\text{cm}^2$ . Upon addition of sodium to the lithium-ion electrolyte, a Li–Na alloy was deposited (mA/cm<sup>2</sup> current density range) that appears to suppress dendrite formation. © 2006 The Electrochemical Society. [DOI: 10.1149/1.2199444] All rights reserved.

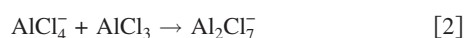
Manuscript submitted August 15, 2005; revised manuscript received January 27, 2006. Available electronically May 15, 2006.

There is interest in higher power and energy density batteries to meet the needs of the electronics and automobile applications while still maintaining durability and safety. Lithium metal-based batteries are desirable because the anode potential is more negative and the atomic weight is lower than intercalation anodes. However, anodes using lithium metal are prone to forming dendrites when recharged, leading to capacity fading and electrode shorting. Large spatial separation between the anode and cathode results in large resistive losses and low current density. The suppression of dendrites is crucial for secondary lithium metal-based batteries.<sup>1</sup>

The formation of dendrites occurs with other metals, such as in the electrodeposition of tin, silver, and zinc.<sup>2–4</sup> Electronic-system failures have been attributed to short circuits caused by metallic dendrites. The silver and tin whiskers observed in electronic components grow slowly over time when the circuit elements are maintained at different potentials. In general, dendrite suppression has been achieved by alloying the metal with a small amount of a second metal, ca. > 1%. For example, tin–lead and zinc–nickel are reliable metal systems for solderability and corrosion resistance.<sup>5,6</sup> The deposition potential and melting point of the alloy are often lower due to the alloy effect.

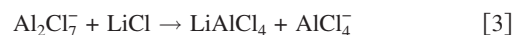
In this work, the lithium alloy has been investigated as a means of producing a dendrite-free anode for lithium batteries. Sodium has been chosen as the alloying metal, although other elements can also be considered, such as potassium. Chloroaluminate ionic liquids (ILs) have been shown to provide an electrolytic medium by which both lithium and sodium can be electrodeposited.<sup>7–10</sup> ILs in general are desirable because they are liquid at (or near) ambient temperature, nonflammable, have near-zero vapor pressure, and substantial ionic conductivity.<sup>11</sup>

A variety of chloride salts (Lewis base) can be mixed with  $\text{AlCl}_3$  (Lewis acid) to form a cation and  $\text{AlCl}_4^-$  anion. For example,  $\text{NaAlCl}_4$  has been used as the electrolyte in the sodium metal anode, referred to as the Zebra Cell.<sup>12</sup> When an organic chloride salt [such as imidazolium or quaternary ammonium chloride (QuatCl)] is used in place of the sodium chloride, depending on the size and symmetry of the resulting cation, a liquid that melts near or below ambient temperature can result.<sup>11</sup> Mixing the organic chloride with excess  $\text{AlCl}_3$  results in an IL with residual acidity.<sup>13</sup> The acidity makeup of the melt is represented by the mole fraction ( $N$ ) of the Lewis acid,  $\text{AlCl}_3$



In an acidic melt, the negative potential is limited by reduction of  $\text{Al}_2\text{Cl}_7^-$  to elemental aluminum.<sup>14</sup> The excess acidity can be neutral-

ized by addition of NaCl or LiCl, providing the sodium and/or lithium ions for electrodeposition.<sup>15</sup> Excess NaCl or LiCl also buffers the ionic liquid to maintain neutrality during deposition



Quaternary ammonium salts have been shown to form ILs with a wide electrochemical stability range.<sup>11</sup> However, studies have shown that it is necessary to have an additive such as  $\text{SOCl}_2$  or HCl in the neutral IL to facilitate the reduction of lithium and sodium cations to the metal.<sup>16,17</sup> It was found that the additives play a role in weakening the bond strength between the cation ( $\text{Na}^+$  and  $\text{Li}^+$ ) and  $\text{AlCl}_4^-$ .<sup>18</sup>

In this paper, the formation of dendrites for lithium, sodium, and their alloys were investigated in an IL electrolyte. The deposition potential, coulombic efficiency for the reoxidation of the deposited metal, and composition of the deposit are reported. Figure 1 shows two QuatCl's, benzyldimethylethylammonium chloride (BMECl), and butyldimethylpropylammonium chloride (BMPCl), utilized to form ILs. BMECl-based chloroaluminate ILs have a low melting point (13.4°C) and acceptable viscosity at room temperature (278 cP).<sup>11</sup> Also,  $\text{BME}^+$  has a reduction potential near  $-2.8$  V vs a saturated calomel reference electrode (SCE) that is sufficient to electrodeposit lithium and sodium. Optical tests were performed using BMP chloroaluminate ILs which have lower viscosity and greater transparency than the BME ILs.<sup>19</sup>

### Experimental

BMECl, was synthesized from benzyl chloride and dimethylethylamine. BMPCl was synthesized from propyl chloride and butyldimethyl amine.<sup>11</sup> BMECl, BMPCl, NaCl (99.999%, Alfa Aesar), and LiCl (99.999%, Alfa Aesar) were dried under vacuum for a

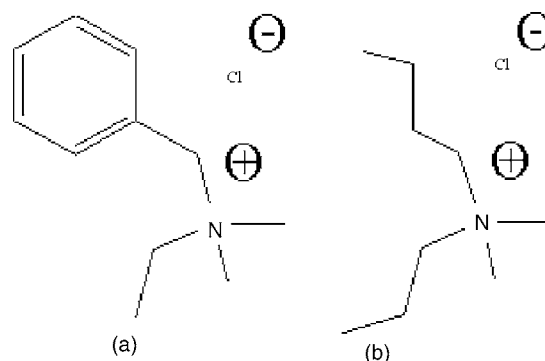


**Figure 1.** Quaternary ammonium salts: (a) benzyldimethylethylammonium chloride (BMECl) and (b) butyldimethylpropylammonium chloride (BMPCl).

\* Electrochemical Society Student Member.

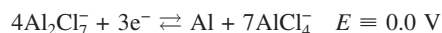
\*\* Electrochemical Society Fellow.

z E-mail: pkohl@bellsouth.net

minimum of 48 h at  $\sim 70^\circ\text{C}$  before being placed in the glove box. Anhydrous ethylene (99%) and propylene carbonate (99.7%), aluminum chloride (99.99%), and thionyl chloride (99 + %) were obtained from Aldrich and put in the glove box as-received. A Vacuum Atmospheres glove box was used to prevent exposure to oxygen and water. The oxygen and water levels were kept below 10 ppm.

A ThermoOrion conductivity meter and a custom-built probe were used to conduct conductivity measurements. Platinum leads were attached to two platinum electrodes that were fabricated, placed in glass, and set apart at a fixed distance. Before every use in the glove box, the conductivity meter was calibrated with a standard NaCl solution (Orion). The probe was cleaned with  $\text{HNO}_3$ , rinsed with deionized (DI) water, and dried in an oven prior to calibration.

Electrochemical measurements were performed by using an EG&G model 273 potentiostat. Pt (99.999%) and W (99.95%) wires were purchased from Alfa Aesar. The working electrodes fabricated by sealing the wires in glass tubes. The electrodes were cleaned with  $\text{HNO}_3$  before each use. Alumina powder was used to polish the electrode surface, followed by a thorough rinsing with DI water prior to use. The reference electrode was formed by immersing an aluminum wire in an acidic melt ( $N = 0.6$ ) in a glass tube that was separated from the electrolyte by a fine glass frit. The following is the cell equation for the reference electrode



When neutralizing the melt, various ratios of LiCl/NaCl were added to the acidic melt at a 20% excess to ensure that neutrality was achieved while maintaining a consistent  $\text{Li}^+/\text{Na}^+$  relation. The electrolytes were then stirred for at least 10 h to make certain neutrality was reached. In order to maintain neutrality of the electrolyte, it was important to perform thorough mixing immediately prior to experimentation. Approximately 0.5 mol % thionyl chloride was added using a micropipette and the melt was stirred for 15 min immediately before running the experiments. Before running the tests, the three electrodes (working, counter, and reference) were placed as close as possible to each other.

The deposits were observed with a custom-built glass cell with an internal cavity less than 1 mm thick. A rectangle Pt foil electrode ( $\sim 0.75 \text{ cm}^2$  area and 0.5 mm thick) was sealed inside the cell on one end. On the opposite end of the cell from the Pt electrode, a small vacuum joint allowed liquid to be pipetted into the cell. The working electrode was formed by sealing a 0.5 mm diam Ni wire in epoxy and polishing the exposed end smooth. The working electrode was then fitted into the joint such that it was in the IL and the liquid was completely sealed from the external environment. Chronopotentiometry (CE) tests were performed under a nitrogen environment with the reference and counter electrodes. An optical microscope and video camera were used to capture images of the electrode surface after deposition.

## Results

The conductivity of the neutral IL containing sodium and/or lithium is of interest because of the degree of ion pairing that occurs between the alkali cation and  $\text{AlCl}_4^-$ . The conductivity of the ILs was measured as a function of the concentration of the dissolved lithium and sodium cations at  $25^\circ\text{C}$ . The mole fraction of  $\text{BME}^+$ , and  $\text{AlCl}_4^-$ , and  $\text{SOCl}_2$  was held constant in all the experiments. The conductivity values for five, neutral ILs with and without  $\text{SOCl}_2$  are shown in Table I. The mole fraction of the alkali cation in the liquid phase was 9 mol % in each IL. The conductivity of the IL increased as the lithium-to-sodium ion ratio increased. The lithium-only ion IL had a conductivity of  $549 \mu\text{S}/\text{cm}$  while the sodium-only IL had a conductivity of  $321 \mu\text{S}/\text{cm}$ . Previously, it was shown that replacement of the organic cations with sodium ions results in a lower conductivity melt due to ion-pairing of  $\text{Na}^+$  with  $\text{AlCl}_4^-$ .<sup>18</sup> The improvement in conductivity by replacement of lithium ions for sodium ions may be due to the smaller size of the lithium ion. A smaller ion could result in a higher packing density along with a greater mobility, resulting

**Table I. Conductivities of neutral ILs.**

| LiCl (%) | NaCl (%) | Before adding $\text{SOCl}_2$<br>Conductivity<br>( $\mu\text{S}/\text{cm}$ ) | After adding $\text{SOCl}_2$<br>Conductivity<br>( $\mu\text{S}/\text{cm}$ ) |
|----------|----------|--|---|
| 100      | 0        | 549  | 542   |
| 90       | 10       | 466  | 469   |
| 50       | 50       | 428  | 466   |
| 10       | 90       | 364  | 371   |
| 0        | 100      | 321  | 363   |

in an increase in conductivity. The conductivity of the LiCl-neutralized melt may also be higher than that of the NaCl melt due to a higher molar saturation for  $\text{Li}^+$  than  $\text{Na}^+$  (i.e., some of the excess LiCl could dissolve). To ensure neutrality of the melt, excess LiCl and/or NaCl was added (depending on the desired melt composition). If a higher percentage of the excess LiCl was dissolved, relative to that of the NaCl, a higher conductivity would be observed due to the greater ion density of the melt.

Additives also affect the conductivity of the melts. Thionyl chloride ( $\text{SOCl}_2$ ) has been shown to increase the conductivity by increasing the degree of dissociation of the  $\text{Li}^+$  and  $\text{Na}^+$  from their counterions, allowing electrodeposition to occur.<sup>18</sup> The  $\sim 10\%$  increase in the conductivity of the Na-only melt (and little change in the Li-only melt) implies that the  $\text{SOCl}_2$  increases the free  $\text{Na}^+$  concentration more than for  $\text{Li}^+$ . The mixed melts show a small increase in conductivity after  $\text{SOCl}_2$  was added. Because the  $\text{SOCl}_2$  is neutral and its molar fraction is small, the liquid itself has little influence on the overall conductivity.<sup>18</sup>

Cyclic voltammetry (CV) was used to characterize the electrodeposition and reoxidation of sodium and lithium. Figure 2 shows CVs for five ILs with different sodium-to-lithium ratios. In each case, the IL had an acidity of  $N = 0.55$  before neutralization.

The reduction potential of the IL neutralized with only NaCl has previously been reported to be  $-2.3 \text{ V}$ .<sup>13</sup> The sodium-containing IL reduction potential is more negative than that of the IL neutralized with LiCl, which begins to reduce at  $-1.8 \text{ V}$ . In each case, a hysteresis was observed where an overpotential for nucleation of the metal was present on the first scan to negative potentials. The 90%  $\text{Li}^+ / 10\% \text{ Na}^+$  IL has a similar current-voltage ( $I$ - $V$ ) behavior to that of the lithium-only IL, and the 10%  $\text{Li}^+ / 90\% \text{ Na}^+$  IL is similar to the sodium-only IL.

The reoxidation of the metal is different for each mixture in Fig. 2. The pure sodium and pure lithium ILs have one large oxidation peak, while the mixed sodium-lithium deposits have two or three oxidation peaks. This is possibly due to the presence of different Li-Na alloys (different ratios of metal), or the selective oxidation of

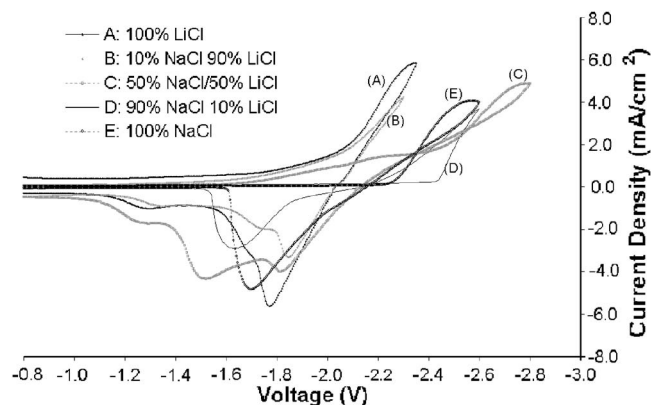


**Figure 2.** CVs of the BMECl: $\text{AlCl}_3$  neutralized melts with 0.5%  $\text{SOCl}_2$  on a Pt electrode referenced with BMECl: $\text{AlCl}_3$  ( $N = 0.6$ ).

**Table II. Coulombic efficiencies.**

| LiCl (%) | NaCl (%) | Cyclic voltametry           |   | Chronoamperometry           |   | Chronopotentiometry         |   |
|----------|----------|-----------------------------|---|-----------------------------|---|-----------------------------|---|
|          |          | Efficiency (%) <sup>a</sup> | Max. efficiency (%)<br>(Switching potential, V) | Efficiency (%) <sup>b</sup> | Max. efficiency (%)<br>(Potential steps, V) | Efficiency (%) <sup>c</sup> | Max. efficiency (%)<br>(Current steps, MA/cm <sup>2</sup> ) |
| 100      | 0        | 72                          | 74 (-2.4)                                       | N/A                         | 62 (-2.35/-1.2)                             | 50                          | 75 (1.02:-1.02)   |
| 90       | 10       | 84                          | 88 (-2.3)                                       | 31                          | 91 (-2.3/-1.3)                              | 40                          | 80 (1.02:-1.02)   |
| 50       | 50       | 83                          | 87 (-2.4)                                       | 46                          | 68 (-2.4/-1.3)                              | 62                          | 65 (0.41:-0.41)   |
| 10       | 90       | 74                          | 74 (-2.6)                                       | 63                          | 72 (-2.45/-1.3)                             | 65                          | 65 (0.51:-0.51)   |
| 0        | 100      | 78                          | 78 (-2.6)                                       | 71                          | 71 (-2.5/-1.8)                              | 85                          | 85 (0.51:-0.51)   |

<sup>a</sup> Switching potential was -2.6 V.

<sup>b</sup> Voltage step to -2.5 and -1.2 V.

<sup>c</sup> Potential steps of  $\pm 0.51$  and  $-0.51$  mA/cm<sup>2</sup>.

one metal from the alloy at a more negative potential than the other metal. For example, the oxidation potential of pure sodium is different from pure lithium metal. A less negative oxidation potential will prevent any reaction between the metal and the organic cation (BME<sup>+</sup>) that is reduced at -2.8 V.

The CV curve for the 50% Li<sup>+</sup>/50% Na<sup>+</sup> is shown in Fig. 2. The slope of the I-V curve is more gradual than the other melts, indicating possible kinetic effects. The reoxidation of the metal shows the most distinct double oxidation peaks of all the alloys studied here. A significant oxidation current is observed at potentials negative of the initial reduction values, indicating that both lithium and sodium are reduced, with lithium at a more positive potential. The sodium is expected to be oxidized first (having a more negative reduction potential) from the alloy.

The coulombic efficiencies for the deposition-stripping of the metal was obtained from the CV curves by integrating the total charge on reduction and oxidation, as reported in Table II. The coulombic efficiency is the total oxidation charge divided by the reduction charge. The first column of results in Table II shows the coulombic efficiencies from the CV experiments when a -2.6 V switching potential was used. The 90% LiCl/10% NaCl IL had the highest efficiency, 84%, and the 50% LiCl/50% NaCl melt had an efficiency of 83%. This is consistent with the previous observation that alloy deposition occurs at more positive potentials, where there is a lower probability of IL reduction. A survey of conditions was performed to find the highest coulombic efficiency in each BME IL. In these experiments, the scan rate was held constant at 100 mV/s while the switching potential was varied. The second column of Table II shows the highest efficiency obtained from the survey experiments along with its corresponding switching potential. The 90% LiCl/10% NaCl melt had the highest efficiency at 88% (switching potential of -2.3 V). The pure lithium IL had an efficiency of 74% (switching potential -2.4 V) while the pure sodium melt had an efficiency of 78% (switching potential -2.6 V). This is consistent with the observation that lithium is deposited at more positive potentials than sodium. The optimal switching potential for the 90% LiCl/10% NaCl melt is similar to that of the 100% LiCl melt. This is consistent with the data in Fig. 2 which shows a similar I-V behavior for the two ILs.

Chronoamperometry (CA) was also used to measure the coulombic efficiency, as shown in Table II. When the efficiency is measured by CV, the potential varies throughout the experiment. The current corresponding to metal deposition vs that corresponding to IL reduction is a function of potential, especially at the extremes of the potential scans. In CA, potential steps are used which correspond more closely to that of a battery's operation. The reduction and oxidation potential steps used in the experiments were varied to find the optimal setting for deposition in each of the ILs. The 90% LiCl/10% NaCl melt had the highest efficiency, 91%, with potential steps of -2.3 V followed by -1.3 V (each step was for 100 s). The 90%

LiCl/10% NaCl melt also gave the highest efficiency from CV measurements. The CA curve for the 90% LiCl/10% NaCl melt can be seen in Fig. 3.

Constant potential steps and step times were applied to each melt to compare the melt efficiencies directly. The efficiency should increase as the amount of metal plated was increased. This was previously shown to be true in other ILs and was attributed to an initial parasitic current due to the reduction of impurities.<sup>17</sup> Potential steps of -2.5 and -1.2 V (100 s per run) were applied to each melt. The efficiency values of each IL subjected to the same potential steps (-2.5 V/-1.2 V) can be seen in Table II in the first chronoamperometry efficiency column. The 100% LiCl IL efficiency is not reported because the potential step to -2.5 V is beyond the stable range of the mixture. The general trend in the maximum efficiencies follows a trend similar to the CV data.

CE was also used to measure the coulombic efficiency. The maximum efficiency was measured by optimizing conditions to maximize the efficiency for each IL. These results are shown in Table II. The values of efficiency are similar to those observed by the other techniques. The 90% LiCl/10% NaCl, which gave the highest efficiency values with CV and CA, had a coulombic efficiency of 80% when the current steps were 1.0 mA/cm<sup>2</sup> for 100 s. The current steps for maximum efficiency were higher in the ILs with high lithium concentration. This can be seen in the CVs in Fig. 2 during deposition where at lower overpotentials there is less competition from reduction of the IL. The current steps required for maximum efficiency for a CE measurement, depending on the melt, ranged from 0.41 to 1.22 mA/cm<sup>2</sup>, as seen in Table II. Each melt was then directly compared by subjecting each IL to current steps of 0.51 mA/cm<sup>2</sup> for 100 s per step. These results are seen in Table II

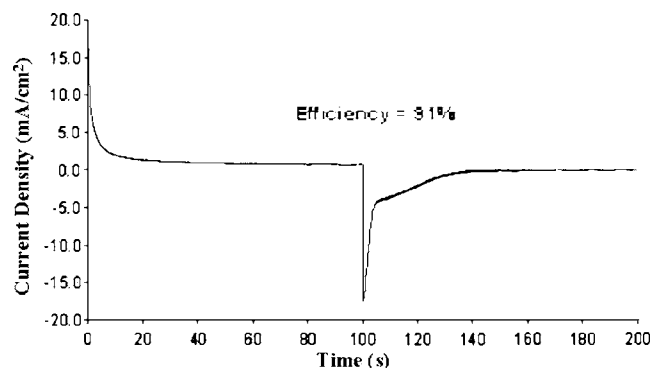


**Figure 3.** Chronoamperometry of the BMECl:AlCl<sub>3</sub> melt ( $N = 0.55$ ) neutralized with excess 90% LiCl/10% NaCl on a Pt electrode at 25°C with SOCl<sub>2</sub> added. Potential steps of -2.3 V followed by -1.3 V were applied.



**Figure 4.** Photograph of lithium deposited on nickel at  $1.53 \text{ mA/cm}^2$  for 30 min from a chloroaluminate BMPCl IL (4 $\times$  magnification).

and show that at a relatively low current, like  $0.51 \text{ mA/cm}^2$ , ILs with higher sodium concentrations have a higher efficiency.

Elemental analysis was performed on the metal deposits for each of the melts in order to determine if both lithium and sodium were present. Atomic absorption spectroscopy and a qualitative flame test were used to determine the presence of lithium and sodium in the deposits. The metal from the electrochemical depositions was initially dissolved in DI water. A platinum wire was immersed in the metal-containing solution and then placed into a blue flame. Sodium and lithium ions produce yellow and red flames, respectively. The pure sodium IL produced a deposit which resulted in a yellow flame and the lithium IL produced a deposit which resulted in a red flame. When the  $\text{Li}^+/\text{Na}^+$  alloy deposits were tested, the flame color was clearly a mixed yellow and red flame. This qualitative analysis confirmed the presence of lithium and sodium deposit from the mixed  $\text{Li}^+/\text{Na}^+$  IL. Atomic absorption was used to quantify the alloy ratio deposited from the 90% Li/10% Na IL. Standard solutions of LiCl and NaCl were prepared and used to calibrate the atomic absorption spectrometer. The electrodeposited metal was dissolved in DI water and the concentration of the two ions was measured. The Na-to-Li ratio obtained by atomic absorption was compared to that in the melt. A Na/Li molar ratio of 50:1 was found from metal deposited from the BMECl IL. This ratio is not consistent with the composition of the melt, indicating that the deposit was sodium-rich; however, quantitative dissolution of the metal deposit may not have occurred. This result clearly shows that Li/Na alloys are present during deposition, resulting in the changes of the electrochemical properties discussed earlier.

Visual examination of the deposits for dendrite formation was performed using a custom-built optical cell. This cell was thin so that visual observations could be made through the IL without disturbing the working electrode. CE tests were performed using a nickel electrode (0.5 mm diam) and BMP IL, which was found to be more transparent than the BME IL. Initially, a constant reduction current of  $1.53 \text{ mA/cm}^2$  was applied for 2.5 min. Following deposition, the open-circuit voltage of the working electrode (relative to the counter electrode) was between  $-3.3$  and  $-4$  V. A constant oxidation current of  $1 \text{ mA/cm}^2$  was then applied until a sharp increase in the voltage was observed, indicating the oxidative removal of the alkali metal. Reduction ( $1.53 \text{ mA/cm}^2$ ) was performed for 30 min followed by examination under a microscope.

Figure 4 shows the dendrite formation from an IL containing only LiCl (no sodium ions present). Dendrites are clearly visible in all depositions from lithium-only ILs. This is consistent with previous findings where dendrites were seen at currents as low as  $0.5 \text{ mA/cm}^2$  in as short as 1 min.<sup>20</sup> When the tests were repeated with a 50/50 wt % mixture of LiCl and NaCl neutral ILs, no dendritic growth was observed. The NaLi alloy deposit was thin and smooth on the surface of the electrode. The electrodes were thoroughly examined for dendrites. The potential of the working electrode was  $-3.65$  V vs the counter electrode at open circuit. This shows that alkali deposit was present on the surface. The application of an oxidation current of  $1 \text{ mA/cm}^2$  for 1 min resulted in a voltage consistent with the oxidation of alkali metal from the surface. The open-circuit voltage was  $-3.55$  V following this test. Finally, im-

mersion of the alkali metal electrode in water resulted in a visible reaction and formation of gas bubbles, consistent with the reaction of elemental lithium or sodium with water.

Extending the deposition time to 4 h resulted in a thicker, rough deposit in each IL. While the Li/Na deposit had a rougher but non-dendritic surface, the lithium-only IL showed the preferential growth of dendrites.

The ability of codeposited sodium to suppress the growth of dendrites was also investigated by dissolving  $\text{LiClO}_4$  and  $\text{NaClO}_4$  (1 M) in ethylene carbonate/propylene carbonate (50:50 vol %). When only 1 M  $\text{LiClO}_4$  was used in the electrolyte, dendritic growth was observed upon deposition for 5 h. When a 50:50 vol % mixture of 1 M  $\text{LiClO}_4$  and 1 M  $\text{NaClO}_4$  was used, a spongy, porous deposit was formed.

## Discussion

The goal of this work was to deposit a Li–Na alloy which could be used as the anode in an alkali metal battery without the formation of dendrites during deposition. Shifts in reduction potentials and oxidation peaks are consistent with alloy deposition. A reduction potential shift occurred during deposition for all the mixed  $\text{Na}^+/\text{Li}^+$  ILs, indicating alloy deposition. Studies have shown that the deposition of two or more metals (in this case, lithium and sodium) is possible as long as the reduction potentials are similar.<sup>4</sup> Figure 2 shows that the pure lithium and pure sodium I–V curves are similar in shape and potential from  $-2.15$  to  $-2.32$  V. The 90% Li/10% Na IL clearly exhibits reduction in this potential range. Chemical analysis confirms the presence of sodium and lithium in the deposit.

The overpotential exhibited during oxidation of the 90% LiCl and 10% NaCl melt deposit is consistent with the existence of an alloy. On positive-going sweeps, oxidation begins at  $-2.0$  V, which is  $0.2$  V more negative than the point of initial reduction ( $-1.8$  V). This could be due to the presence of an alloy or selective oxidation of one metal from the alloy at a more negative potential. Other studies have shown that two-phase alloys can codeposit on a polarized electrode surface even if a system is capable of forming a continuous solid deposit.<sup>4</sup> Multiphase alloys can produce the multiple oxidation peaks, as seen in our results.

Like lithium, both silver and tin form dendrites in the presence of a potential gradient. Dendritic growth with silver and tin is suppressed by alloy formation. Similarly, dendrite formation was observed when the deposition was carried out at  $1.5 \text{ mA/cm}^2$  for 30 min in a LiCl neutral IL. When a mixed (LiCl and NaCl) neutral IL was used under the same conditions, dendrite formation was not observed. Further studies are necessary to determine the optimal conditions and composition for preventing dendritic growth. Parameters such as concentration and current density must be examined for use as a Li–Na alloy anode.

A rechargeable Li-ion battery consists of a lithium anode and a metal oxide cathode such as lithium cobalt oxide.<sup>21</sup> To maximize the specific capacity of the battery, the minimum sodium concentration at which a nondendritic deposit is formed should be used. Also, the amount of sodium should be minimized as the cathode works on the lithium-only cycle, making it necessary for the electrolyte to hold the entire  $\text{Na}^+$  content when the battery is discharged. For example, the minimum sodium content to suppress dendrites needs to be understood to operate in a battery with a metal anode and oxide cathode (e.g.,  $\text{MnO}_2/\text{Li}_x\text{MnO}_2$ ). The sodium would participate in the anode reaction but not with the cathode (to an appreciable extent). During charging, the majority of the sodium would reside in the metallic state on the anode and maintain a minimum content so as to suppress dendrite growth. During discharge, the lithium would reside in the metal oxide (e.g.,  $\text{Li}_x\text{MnO}_2$ ) and a majority of the sodium ions would be dissolved in the electrolyte. Thus, the volume of electrolyte, solubility of sodium ions, and minimum sodium content in the alloy to suppress dendritic growth are intimately related.

### Acknowledgment

The authors gratefully acknowledge the support of the U.S. Department of Energy, contract DE-FG)@-02ER15328, under the direction of Dr. Paul Maupin.

Georgia Institute of Technology assisted in meeting the publication costs of this article.

### References

1. J. O. Besenhard, *Handbook of Battery Materials*, Wiley-VCH, Weinheim (1999).
2. J. Diggle, A. Despic, and J. O'M. Bockris, *J. Electrochem. Soc.*, **115**, C228 (1968).
3. M. Rohnke, T. Best, and J. Janek, *J. Solid State Electrochem.*, **9**, 239 (2005).
4. Y. Zhang and A. Ays, *Modern Electroplating*, 4th ed., John Wiley & Sons, Inc., New York (2000).
5. M. Kamitani, T. Koga, and H. Tsuji, *Plat. Surf. Finish.*, **72**, 31 (1985).
6. D. Tench and D. Anderson, *Plat. Surf. Finish.*, **77**, 44 (1990).
7. J. Wilkes, J. Levisky, R. Wilson, and C. Hussey, *Inorg. Chem.*, **21**, 1263 (1982).
8. G. Gray, J. Winnick, and P. Kohl, *J. Electrochem. Soc.*, **143**, 3820 (1996).
9. T. Riechel and J. Wilkes, *J. Electrochem. Soc.*, **139**, 977 (1992).
10. C. Yu, J. Winnick, and P. Kohl, *J. Electrochem. Soc.*, **138**, 339 (1991).
11. K. Kim, C. Lang, and P. Kohl, *J. Electrochem. Soc.*, **152**, E56 (2005).
12. R. Bones, J. Coetzer, R. Galloway, and D. Teagle, *J. Electrochem. Soc.*, **134**, 2379 (1987).
13. K. Kim, C. Lang, R. Moulton, and P. Kohl, *J. Electrochem. Soc.*, **151**, A1168 (2004).
14. C. Scordilis-Kelley, J. Fuller, R. Carlin, and J. Wilkes, *J. Electrochem. Soc.*, **139**, 694 (1992).
15. T. Melton, J. Joyce, J. Maloy, J. Boon, and J. Wilkes, *J. Electrochem. Soc.*, **137**, 3865 (1990).
16. J. Fuller, R. Osteryoung, and R. Carlin, *J. Electrochem. Soc.*, **142**, 3632 (1995).
17. G. Gray, P. Kohl, and J. Winnick, *J. Electrochem. Soc.*, **142**, 3636 (1995).
18. K. Kim, C. Lang, and P. Kohl, *J. Electrochem. Soc.*, **152**, E9 (2005).
19. C. Lang, K. Kim, L. Guerra, and P. Kohl, *J. Phys. Chem. B*, **109**, 19454 (2005).
20. J. Yamaki, S. Tobishima, K. Hayashi, K. Saito, Y. Nemoto, and M. Arakawa, *J. Power Sources*, **74**, 219 (1998).
21. Y. Kim, H. Kim, B. Kim, D. Ahn, J. Lee, T. Kim, D. Son, J. Cho, Y. Kim, and B. Park, *Chem. Mater.*, **15**, 1505 (2003).